



# Multi-user bidirectional communication using isochronal synchronisation of array of chaotic directly modulated semiconductor lasers

Bindu M. Krishna<sup>a,\*</sup>, Manu P. John<sup>b</sup>, V.M. Nandakumaran<sup>b,1</sup>

<sup>a</sup> Sophisticated Test and Instrumentation Centre, Cochin University of Science and Technology, Cochin-682022, Kerala, India

<sup>b</sup> International School of Photonics, Cochin University of Science and Technology, Cochin-682022, Kerala, India

## ARTICLE INFO

### Article history:

Received 2 May 2009

Received in revised form 18 January 2010

Accepted 17 February 2010

Available online 19 February 2010

Communicated by A.R. Bishop

### Keywords:

Isochronal synchronisation

Bidirectional secure communication

Directly modulated semiconductor lasers

Nonlinear dynamics and chaos

## ABSTRACT

Isochronal synchronisation between the elements of an array of three mutually coupled directly modulated semiconductor lasers is utilized for the purpose of simultaneous bidirectional secure communication. Chaotic synchronisation is achieved by adding the coupling signal to the self feedback signal provided to each element of the array. A symmetric coupling is effective in inducing synchronisation between the elements of the array. This coupling scheme provides a direct link between every pair of elements thus making the method suitable for simultaneous bidirectional communication between them. Both analog and digital messages are successfully encrypted and decrypted simultaneously by each element of the array.

© 2010 Elsevier B.V. All rights reserved.

## 1. Introduction

Chaotic synchronisation has emerged as an important topic of research in diverse fields like physical [1], chemical [2] and biological systems [3]. Synchronisation of chaotic lasers has attracted much attention in the recent years for its potential application in single as well as multi-channel secure communication [4–10]. Recently, secure high speed long distance communication is achieved using synchronisation of chaotic lasers [11]. Long wavelength directly modulated semiconductor lasers are the most preferred light source in the fiber-optic communication links due to the appropriateness of its output wavelength which falls in the minimum loss and dispersion window of optical fibers. This has attracted much attention to the study of its chaotic dynamics and synchronisation [12–16]. Dynamics of semiconductor lasers with direct current modulation is also widely investigated [17–21]. A positive delayed optoelectronic feedback combined with strong current modulation suppresses chaotic dynamics and bistability in semiconductor lasers [22,23]. For InGaAsP lasers used in optical communication systems, the gain reduction occurring due to nonlinear processes is very strong and its effect is the suppression of chaotic dynamics [12]. It is recently reported that a negative delayed optoelectronic

feedback is efficient in producing chaotic outputs from directly modulated semiconductor lasers with optimum value of nonlinear gain suppression factor [16].

Synchronization of two chaotic semiconductor lasers can be achieved using many different coupling schemes like unidirectional coupling [24,25], bidirectional coupling [26,27] which can be either optical or optoelectronic, direct or delayed [28,29]. Even though bidirectional coupling is effective in synchronizing chaotic oscillators, all the secure communication systems devised until very recently were mainly based on unidirectional coupling. Message transmission in both directions is the general approach in commercial communication systems. This naturally demands a bidirectional coupling between the oscillators. Also, channel delay is one of the most critical factors that affect the performance efficiency of secure communication systems using coupled chaotic systems. These realizations have enhanced the importance of research on synchronisation of bidirectional delay coupled oscillators [30–38].

Most of the methods proposed for the isochronous (zero-lag) synchronisation of delay coupled systems depend on the introduction of a third relay element coupled bidirectionally to the two oscillators [30–32], where the relay element can even be different from the outer systems [30]. As there is no direct link between the oscillators which are isochronally synchronized, this method has limited applicability for the purpose of bidirectional secure communication. Recent studies have shown that using the third element as a drive element rather than as a relay element [37] can provide isochronal synchronisation between the oscillators and

\* Corresponding author. Tel.: +91 484 2575908; fax: +91 484 2576699.

E-mail address: bindum@cusat.ac.in (B.M. Krishna).

<sup>1</sup> Present address: Indian Institute of Science education & Research, Thiruvananthapuram, CET Campus, Thiruvananthapuram-695016, Kerala, India.

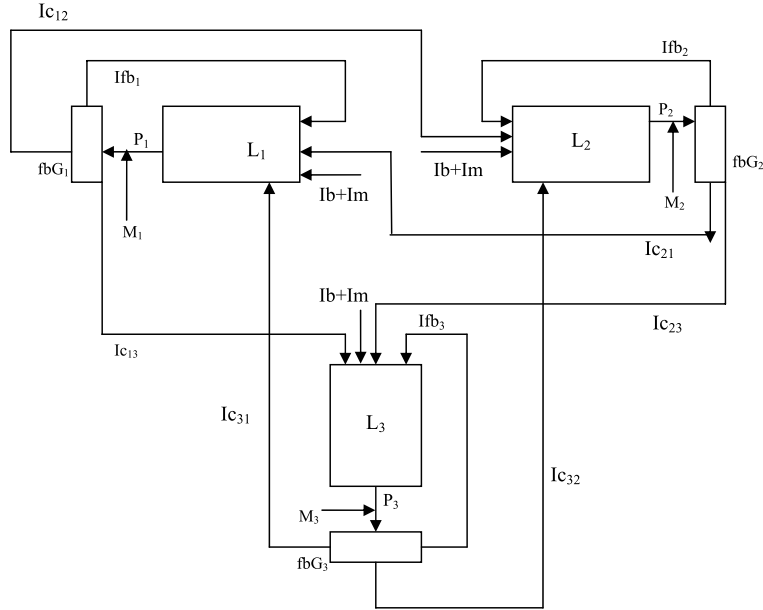


**Fig. 1.** Schematic of array of three mutually delay coupled directly modulated semiconductor lasers with negative optoelectronic feedback. The laser diodes  $L_1$ ,  $L_2$  and  $L_3$  are driven by bias current  $I_b$  and a GHz modulation current  $I_m$ .  $fbG_1$ ,  $fbG_2$  and  $fbG_3$  are feedback generators which splits the light outputs  $P_1$ ,  $P_2$ ,  $P_3$  into required fractions for self feedback and coupling signals delayed by appropriate times and generates proportional feedback signals  $lfb_1$ ,  $lfb_2$ ,  $lfb_3$  and coupling signal  $lc_{12}$ ,  $lc_{13}$ ,  $lc_{21}$ ,  $lc_{23}$ ,  $lc_{31}$ ,  $lc_{32}$  respectively.  $M_1$ ,  $M_2$  and  $M_3$  are message signals which are encoded onto the outputs of  $L_1$ ,  $L_2$  and  $L_3$  by the chaotic masking scheme.

is effective for bidirectional communication. A method of using face to face coupling added with self feedback is also effective in achieving isochronous synchronisation between two chaotic semiconductor lasers [34,35] and has better stability performance when compared to the scheme without self feedback. A performance comparison of unidirectional and bidirectional coupling between chaotic semiconductor lasers with self feedback demonstrating the high tolerance of bidirectional coupling towards parameter mismatch is reported recently [38].

Here we investigate the possibility of bidirectional secure communication in an array of three mutually delay coupled chaotic directly modulated semiconductor lasers. Individual array elements are long wavelength directly modulated semiconductor lasers with optimum values of nonlinear gain reduction factor and delayed optoelectronic self feedback. The method of adding coupling signal to the self feedback signal is used for synchronizing the array elements. Analog and digital messages are successfully encoded and decoded simultaneously at each element. The results show that the method is effective for simultaneous multi-user secure communication in optical communication networks.

## 2. Laser array model

Schematic diagram of the array of mutually coupled directly modulated semiconductor lasers with a delayed negative optoelectronic feedback is shown in Fig. 1. Laser diodes  $L_1$ ,  $L_2$  and  $L_3$  are driven with their bias currents which are modulated using a sinusoidal GHz current and are mutually coupled to each other. A fraction of the light output from each element is delayed by the required time, converted into electronic signal and is fed back to its own input as self feedback signal. Two other fractions are sent to the other two elements as coupling signals. Thus each element receives a total of three delayed feedback signals comprising of the self feedback signal and two coupling signals received from the other two elements. The total feedback signal of every element is kept equal to the optimum value required for producing chaotic outputs [16]. Dynamics of each of the array elements can be represented by rate equations for the photon density ( $P$ ), carrier density ( $N$ ), and driving current ( $I$ ) as follows

$$\frac{dN_{1,2,3}}{dt} = \frac{1}{\tau_e} \left\{ \left( \frac{I_{1,2,3}}{I_{th}} \right) - N_{1,2,3} - \left[ \frac{N_{1,2,3} - \delta}{1 - \delta} \right] P_{1,2,3} \right\} \quad (1)$$

$$\frac{dP_{1,2,3}}{dt} = \frac{1}{\tau_p} \left\{ \left[ \frac{N_{1,2,3} - \delta}{1 - \delta} \right] (1 - \varepsilon P_{1,2,3}) P_{1,2,3} - P_{1,2,3} + \beta N_{1,2,3} \right\} \quad (2)$$

$$I_{1,2,3}(t) = I_b + I_m \sin(2\pi f_m t) - r_s \times (P_{1,2,3}(t - \tau_s)) - r_{c_{2,3,1}} \times (P_{2,3,1}(t - \tau_c)) - r_{c_{3,1,2}} \times (P_{3,1,2}(t - \tau_c)) \quad (3)$$

The subscripts 1, 2, 3 represent the array element address,  $N$  and  $P$  are the carrier and photon densities,  $I$  is the driving current,  $\tau_e$  and  $\tau_p$  are the electron and photon lifetimes,  $\delta = n_0/n_{th}$ ,  $\varepsilon = \varepsilon_{NL} S_0$  are dimensionless parameters where  $n_0$  is the carrier density required for transparency,  $n_{th} = (\tau_e I_{th}/eV)$  is the threshold carrier density,  $\varepsilon_{NL}$  is the factor governing the nonlinear gain reduction occurring with an increase in  $S$ ,  $S_0 = \Gamma(\tau_p/\tau_e)n_{th}$ ,  $I_{th}$  is the threshold current,  $e$  is the electron charge,  $V$  is the active volume,  $\Gamma$  is the confinement factor and  $\beta$  is the spontaneous emission factor.  $I_b = b \times I_{th}$  is the bias current where  $b$  is the bias strength,  $I_m = m \times I_{th}$  is the modulation current where  $m$  is the modulation depth and  $f_m$  is the modulation frequency [12]. The parameters  $r_s$  and  $r_c$  are the self feedback and coupling strengths and  $\tau_s$  and  $\tau_c$  are the feedback and coupling delay times. The total strength of the signal comprising of the self feedback and coupling signals is kept within the optimum value of delayed feedback for producing chaotic outputs [16]. The delay times of coupling and self feedback signals are also fixed at their optimum values. The above equations are numerically simulated using fourth order Runge–Kutta method with parameter values as given in Table 1. For investigating the message encoding/decoding characteristics of the scheme shown in Fig. 1, three message signals  $M_1$ ,  $M_2$  and  $M_3$  are encoded onto the outputs  $P_1$ ,  $P_2$  and  $P_3$  of lasers  $L_1$ ,  $L_2$  and  $L_3$  respectively. These messages are received and decoded simultaneously at the other two lasers.

**Table 1**  
Parameter values used for numerical simulation.

Parameter	Value
$\tau_e$	3 ns
$\tau_p$	6 ps
$\epsilon$	0.05
$\delta$	$692 \times 10^{-3}$
$\beta$	$5 \times 10^{-5}$
$f_m$	0.8 GHz
$I_{th}$	26 mA
$m$	0.55
$b$	1.5
$r$	0.02
$\tau$	3.78 ns

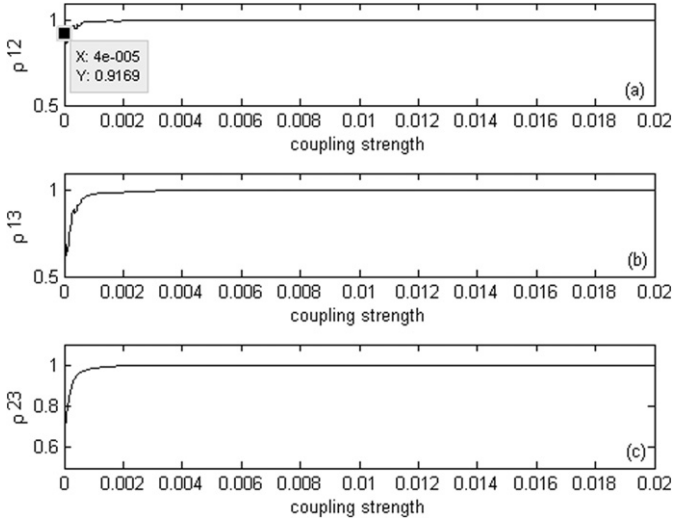


**Fig. 2.** Variation of correlation coefficient with increase in coupling strength for three mutually coupled directly modulated semiconductor lasers. (a)  $\rho_{12}$  between laser pairs  $L_1$  and  $L_2$ ; (b)  $\rho_{13}$  between laser pairs  $L_1$  and  $L_3$ ; (c)  $\rho_{23}$  between laser pairs  $L_2$  and  $L_3$ .

**3. Results and discussion**

To investigate the synchronisation properties of the array, the variation of correlation coefficient between photon densities of each pair of elements with respect to variation in total coupling received by each element is estimated. When the coupling strength is zero the lasers are uncoupled and the self feedback provides the necessary delayed feedback required for producing chaotic outputs. To introduce coupling between the elements, the self feedback of each element is reduced by a certain amount and this is provided equally by the coupling signals received from the two other elements of the array. When the coupling strength becomes equal to that of the total required feedback strength, the self feedback is totally cut off so as to maintain the total delayed feedback in the optimum value limit. Fig. 2(a), (b) and (c) show the variation of instantaneous correlation coefficient between laser pairs  $L_1$  and  $L_2$ ,  $L_1$  and  $L_3$ , and  $L_2$  and  $L_3$  respectively with respect to variation of total coupling received by each element. As the coupling strength increases from zero, the synchronisation quality between the outputs of each pair of elements increases. The correlation coefficient between every pair reaches 0.9 for a coupling strength as low as  $4 \times 10^{-5}$  which further increases for still higher coupling values. The results show that isochronal synchronisation of high quality is achieved between every pair of elements in the array.

Effectiveness of the above scheme for secure communication is investigated using both analog and digital messages. A symmetric coupling is applied between the array elements for this purpose.

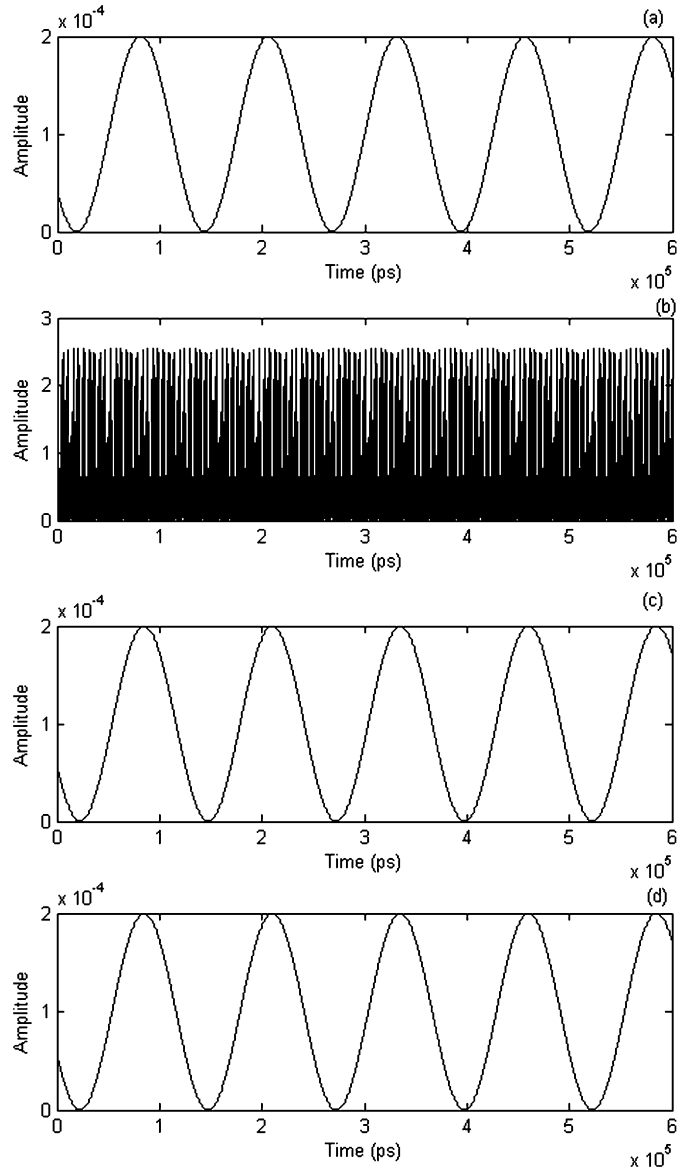


**Fig. 3.** Encoding/decoding of analog message  $M_1$  using chaotic modulation: (a) original message of amplitude  $1e-4$ , modulation index of 0.01; (b) total transmitted signal  $T_1$ ; (c) message  $M_1$  decoded at  $L_2$ ; (d) message  $M_1$  decoded at  $L_3$ .

The total feedback of each element is provided equally by the self feedback signal and two coupling signals received from the other two elements. Each of these fractions is kept equal to one third of the total required feedback. Three different messages are encoded onto the outputs  $P_1$ ,  $P_2$  and  $P_3$  of the three lasers  $L_1$ ,  $L_2$  and  $L_3$  by the chaotic masking scheme. In this scheme the message encoding is done by adding the message signals to the chaotic carriers in such a way that the chaos properly masks the information. Therefore the signals transmitted by each of the three lasers can be represented as

$$T_{1,2,3} = P_{1,2,3} + M_{1,2,3} \tag{4}$$

For ensuring proper masking of the message in the chaos of the carrier signal, the message amplitudes are restricted to  $< 12\%$  of the maximum value of the transmitter output amplitude [15]. For the same reason the modulation index  $m_o = \frac{f_m}{f_{mtr}}$ , the ratio of modulation frequency of the input current of the transmitter to the frequency of message is restricted to  $< 1$ .

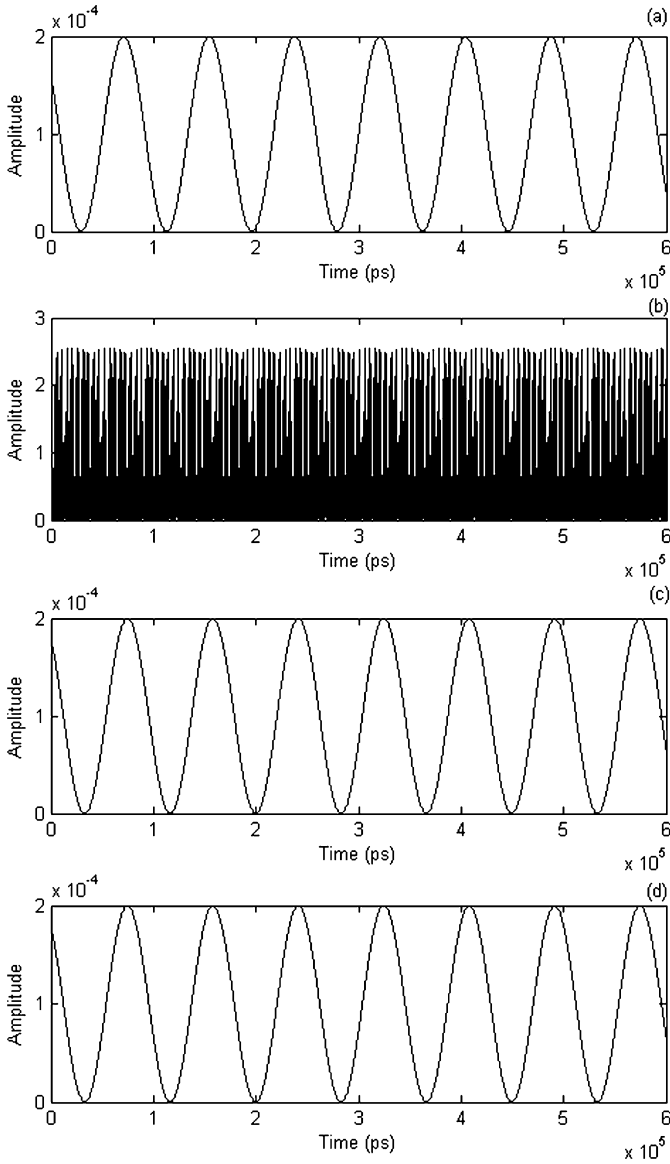


**Fig. 4.** Encoding/decoding of analog message at  $M_2$  using chaotic modulation: (a) original message of amplitude  $1e-4$ , modulation index of 0.015; (b) total transmitted signal  $T_2$ ; (c) message  $M_2$  decoded at  $L_1$ ; (d) message  $M_2$  decoded at  $L_3$ .

Analog messages of three different amplitudes 0.0001, 0.0002 and 0.0003 and modulation indices 0.01, 0.015 and 0.02 are added to each of the outputs  $P_1$ ,  $P_2$  and  $P_3$  of lasers  $L_1$ ,  $L_2$  and  $L_3$ . A fraction of this total signal is transmitted to the two other elements of the array and is also fed back to its own input as its delayed feedback signal. The self feedback delay time and the traveling time of the coupling signal for every element are kept equal. Thus every element will receive a total feedback signal consisting of the transmitted signals of all the three elements containing the corresponding messages in it. Therefore, the total input signal of each element will be modified as follows

$$\begin{aligned}
 I_{1,2,3}(t) = & I_b + I_m \sin(2\pi f_m t) \\
 & - r_s \times (P_{1,2,3}(t - \tau) + (M_{1,2,3}(t - \tau))) \\
 & - \left[ \left( \frac{r_c}{2} \right) \times (P_{2,3,1}(t - \tau) + (M_{2,3,1}(t - \tau))) \right. \\
 & \left. + \left( \frac{r_c}{2} \right) \times (P_{3,1,2}(t - \tau) + M_{3,1,2}(t - \tau)) \right] \quad (5)
 \end{aligned}$$

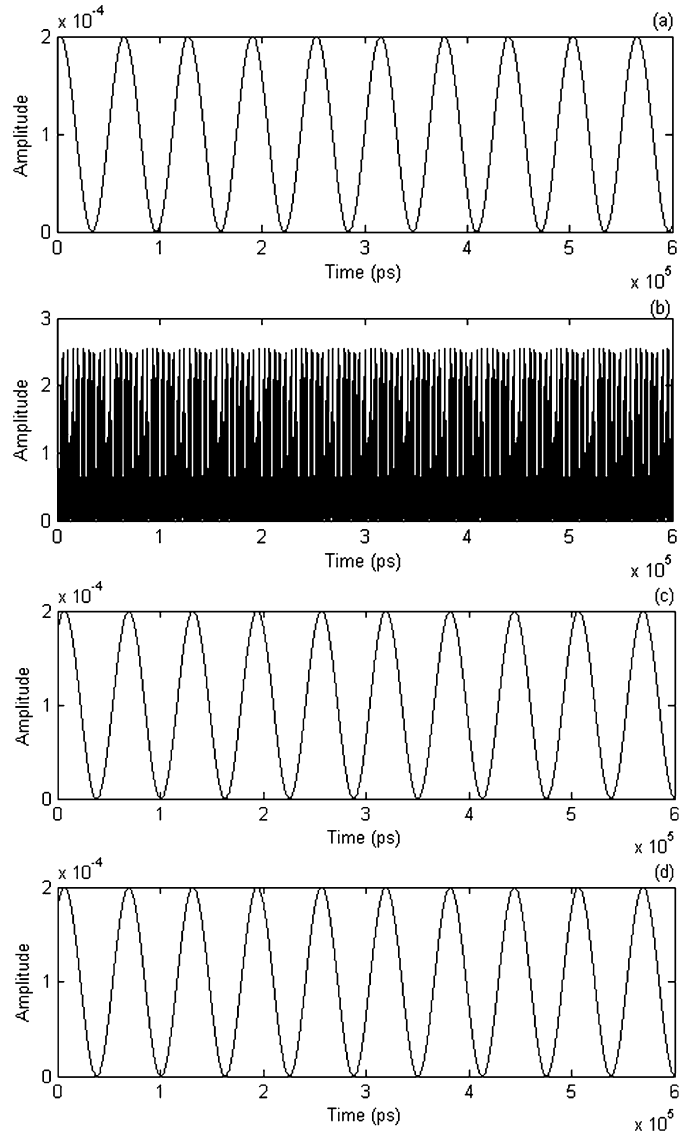


**Fig. 5.** Encoding/decoding of analog message at  $M_3$  using chaotic modulation: (a) original message of amplitude  $1e-4$ , modulation index of 0.02; (b) total transmitted signal  $T_3$ ; (c) message  $M_3$  decoded at  $L_1$ ; (d) message  $M_3$  decoded at  $L_2$ .

Here,  $M$  with subscripts represents the message received from the corresponding elements. Once the lasers are isochronally synchronized, the messages are decoded simultaneously at each element by subtracting the receiver's delayed output from the signal received from each of the other two elements. The decoded messages can be represented as follows

$$\begin{aligned}
 M'_{2,3} = & T_{2,3}(t - \tau) - P_1(t - \tau) \\
 = & [P_{2,3}(t - \tau) + M_{2,3}(t - \tau) - P_1(t - \tau)] \\
 M'_{1,3} = & T_{1,3}(t - \tau) - P_2(t - \tau) \\
 = & [P_{1,3}(t - \tau) + M_{1,3}(t - \tau) - P_2(t - \tau)] \\
 M'_{1,2} = & T_{1,2}(t - \tau) - P_3(t - \tau) \\
 = & [P_{1,2}(t - \tau) + M_{1,2}(t - \tau) - P_3(t - \tau)] \quad (6)
 \end{aligned}$$

In the above equations,  $M'$  with subscripts represents the corresponding decoded messages at the receivers represented by  $P$  with their subscripts. The total signal transmitted by each element is represented by  $T$  with its corresponding subscripts. Thus, messages

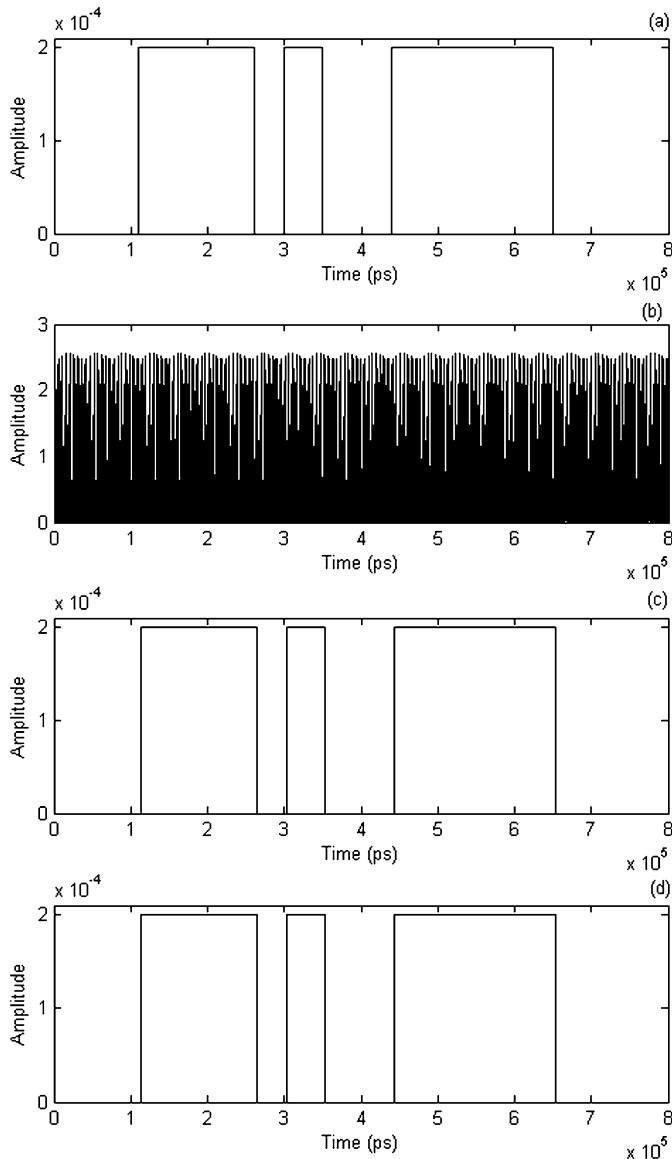


**Fig. 6.** Encoding/decoding of digital message  $M_1$  using chaotic modulation: (a) original message of random bits of amplitude  $2e-4$ ; (b) total transmitted signal  $T_1$ ; (c) message  $M_1$  decoded at  $L_2$ ; (d) message  $M_1$  decoded at  $L_3$ .

$M'_2$  and  $M'_3$  are recovered at  $L_1$  by subtracting  $P_1$  from  $T_2$  and  $T_3$  respectively. Similarly, messages  $M'_1$  and  $M'_3$  are recovered at  $L_2$  and messages  $M'_1$  and  $M'_2$  are recovered at  $L_3$ .

Fig. 3(a) shows the original message  $M_1$  and Fig. 3(b) shows the total signal  $T_1$  comprising of message  $M_1$  and the output  $P_1$  of laser  $L_1$  which is transmitted from  $L_1$  to  $L_2$  and  $L_3$ . Fig. 3(c) and (d) show this message  $M_1$  decoded at  $L_2$  and  $L_3$  respectively. Fig. 4(a) shows the original message  $M_2$  and Fig. 4(b) shows the total signal  $T_2$ . This total signal is transmitted from  $L_2$  to  $L_1$  and  $L_3$  respectively. Fig. 4(c) and (d) show message  $M_2$  decoded at  $L_1$  and  $L_3$  respectively. Fig. 5(a) shows the original message  $M_3$  and Fig. 5(b) shows the total signal  $T_3$ . Fig. 5(c) and (d) show message  $M_3$  decoded at  $L_1$  and  $L_2$  respectively. From the figures it is clear that the messages are completely masked by the chaotic carrier signals. Each of the two messages decoded at every element is found to have all the qualitative features of their original counterparts. These results indicate the high quality decoding provided for all the messages at each of the receiver element.

Similarly digital messages of random bits are encoded onto the outputs of each of the array element. Fig. 6(a), (b), (c) and (d) show

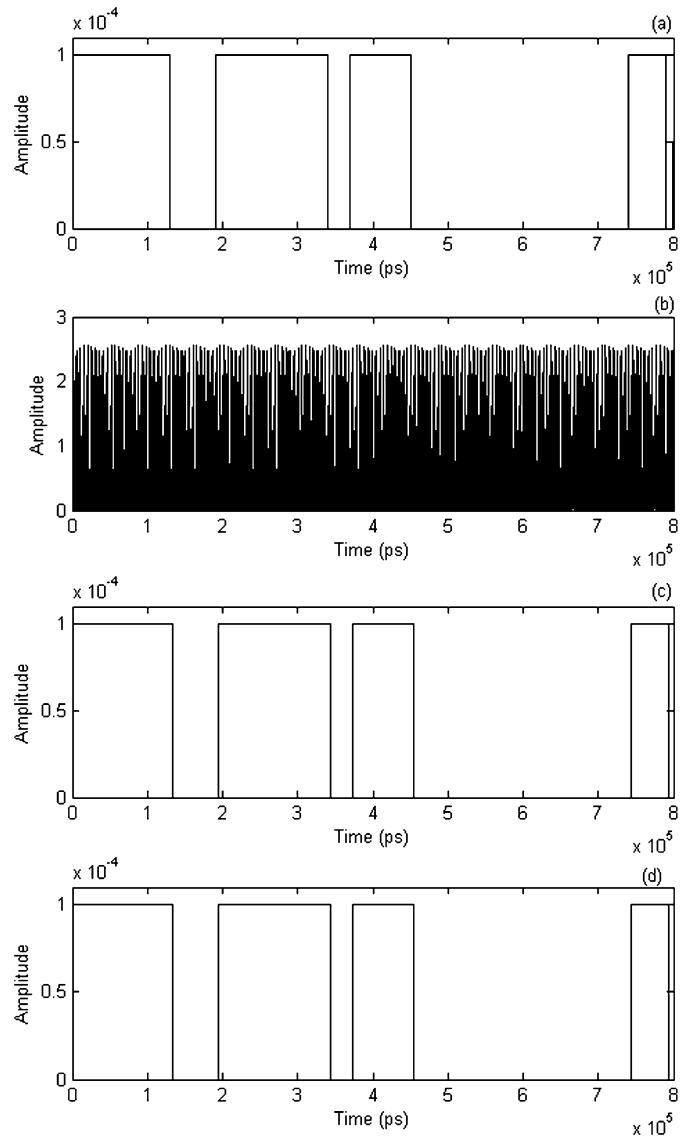


**Fig. 7.** Encoding/decoding of digital message  $M_2$  using chaotic modulation: (a) original message of random bits of amplitude  $1e-4$ ; (b) total transmitted signal  $T_2$ ; (c) message  $M_2$  decoded at  $L_1$ ; (d) message  $M_2$  decoded at  $L_3$ .

the original message  $M_1$  of amplitude 0.0002, the total signal  $T_1$  transmitted from  $L_1$ , and the corresponding decoded messages at  $L_2$  and  $L_3$ . Fig. 7(a), (b), (c) and (d) show the original message  $M_2$  of amplitude 0.0001, the total signal  $T_2$  transmitted from  $L_2$  and the corresponding messages decoded at  $L_1$  and  $L_3$ . Fig. 8(a), (b), (c) and (d) show message  $M_3$  of amplitude 0.0003, total transmitted signal  $T_3$  and  $M_3$  decoded at  $L_1$  and  $L_2$  respectively. It is clear from Figs. 3–8 that this scheme is highly efficient in simultaneous decoding of messages. From these figures, it can also be inferred that the message signals are properly masked by the chaotic carrier waveforms. The periodicity in the envelop of the transmitted signals are due to the inherent property of the waveform which is characteristic of the feedback delay time. The amplitudes and frequencies of the message signals are not evident in the transmitted signals. The dynamic ranges of oscillations of the analog as well as digital messages are between 0 and 0.0003 arbitrary units. The corresponding range of transmitted signal is between 0 and 3 arbitrary units. This confirms that the message signal properties are not visible in the transmitted signal.

To investigate the efficiency of the scheme with respect to asymmetric coupling, quality of each recovered message is esti-

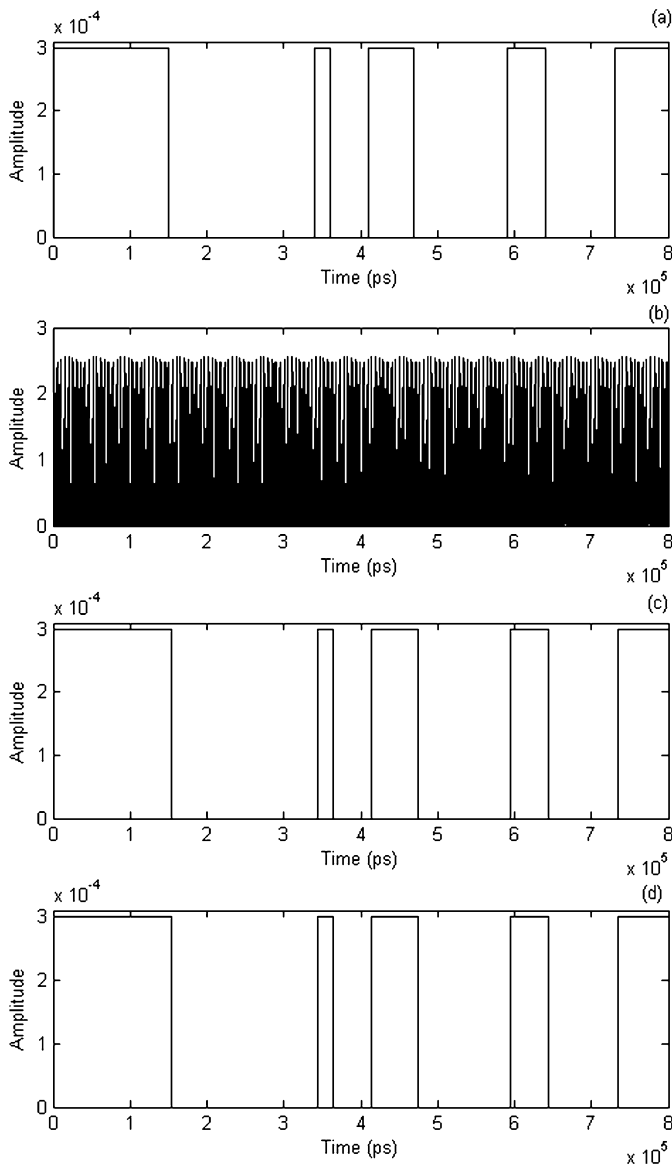


**Fig. 8.** Encoding/decoding of digital message  $M_3$  using chaotic modulation: (a) original message of random bits of amplitude  $3e-4$ ; (b) total transmitted signal; (c) message  $M_3$  decoded at  $L_1$ ; (d) message  $M_3$  decoded at  $L_2$ .

mated for the range of coupling strength same as in Fig. 2. Quality of recovered message is estimated using the correlation coefficient of the recovered message with the original message. Fig. 9(a) and (b) show the variation of decoding quality of message  $M_1$  at lasers  $L_2$  and  $L_3$  respectively with respect to increase in coupling strength received from each of the other two elements. Similarly, Fig. 10(a) and (b) show the variation of decoding quality of message  $M_2$  at lasers  $L_1$  and  $L_3$  respectively and Fig. 11(a) and (b) show the variation of decoding quality of message  $M_3$  at lasers  $L_1$  and  $L_2$  respectively. The decoding quality of each of the three messages increases with increase in coupling strength and reaches a maximum at the coupling strength of 0.00665 which is one third of the total required feedback where the coupling scheme becomes a symmetric one. Even though there are slight differences in values of maximum decoding efficiency of the three messages, the decoding quality remains above 90% for coupling strength between 0.00635 and 0.007 in all three cases. It is found that good correlation between the original message and the messages decoded at either of the two receiver elements are maintained for 4.5% of variation in coupling strengths. It can be inferred from the

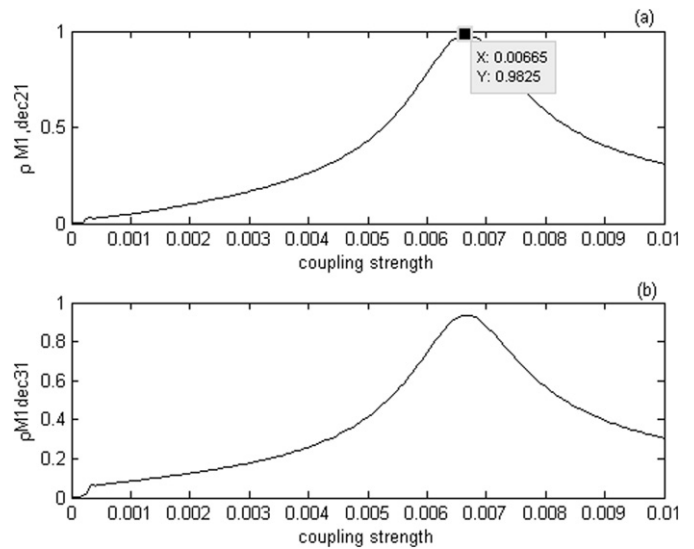


**Fig. 9.** Variation of decoding efficiency calculated as correlation between the original message and decoded message with respect to increase in coupling strength received from each of the two other elements for (a) message  $M_1$  decoded at  $L_2$ ; (b) message  $M_1$  decoded at  $L_3$ .

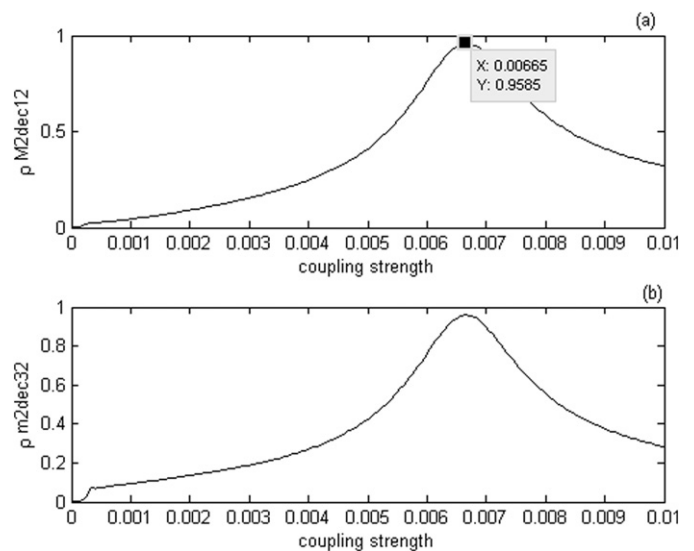


**Fig. 10.** Variation of decoding efficiency calculated as correlation between the original message and decoded message with respect to increase in coupling strength received from each of the two other elements for (a) message  $M_2$  decoded at  $L_1$ ; (b) message  $M_2$  decoded at  $L_3$ .

above results that even though coupling forms other than that of the symmetric one can provide synchronisation, the decoding efficiency drops when the symmetric nature of coupling is changed. This sensitivity of decoding efficiency could be attributed to the stability of synchronisation as effected by the difference in history of lasers which prevents isochronal synchrony [34]. However, further detailed investigations are essential for providing a conclusive explanation of this difference in performance.

To investigate the efficiency of this method in encoding/decoding of real signals, three low amplitude audio signals, viz., a church bell ring  $M_1$ , a toy train horn  $M_2$  and an air horn  $M_3$  are encoded onto the outputs of the three lasers  $L_1$ ,  $L_2$  and  $L_3$  respectively. The audio signals are recorded at 16 bit resolution and 11 kHz sampling rate and the wave files are converted to data files. These signals are encoded onto the chaotic carriers by the chaotic masking scheme. The waveforms are scaled down for proper masking

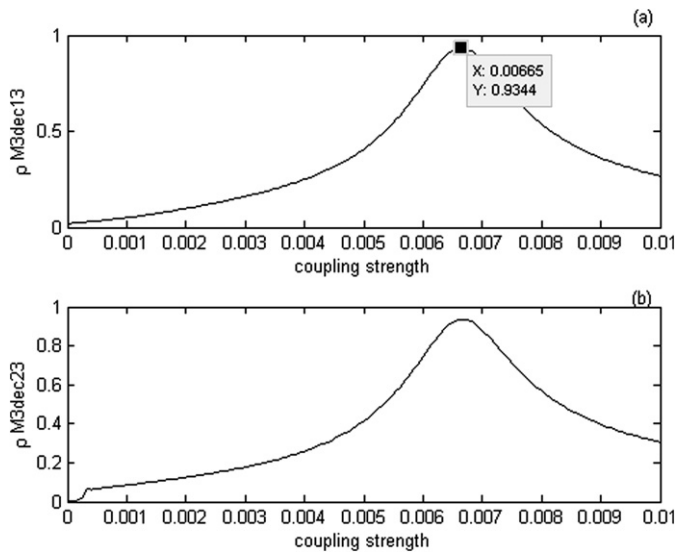


**Fig. 11.** Variation of decoding efficiency calculated as correlation between the original message and decoded message with respect to increase in coupling strength received from each of the two other elements for (a) message  $M_3$  decoded at  $L_1$ ; (b) message  $M_3$  decoded at  $L_2$ .

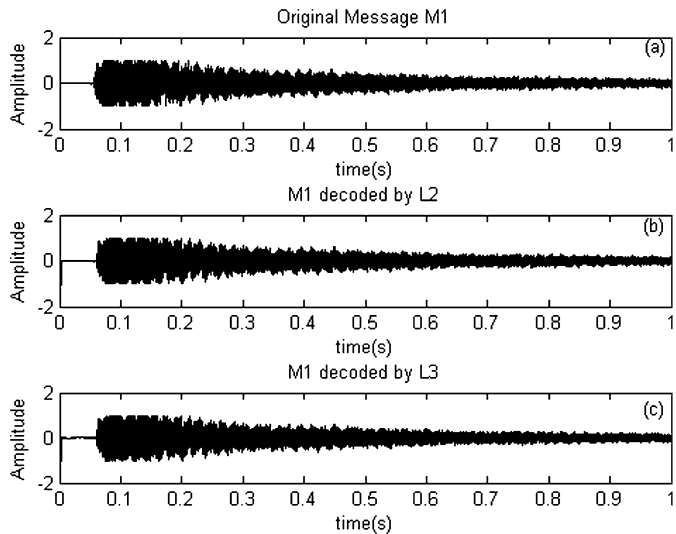


**Fig. 12.** (a) Waveforms of original audio signal of church bell which is encoded as message  $M_1$  onto the chaotic output of the laser  $L_1$ . (b) Waveform of  $M_1$  decoded at  $L_2$ . (c) Waveform of  $M_1$  decoded at  $L_3$ .

in the natural dynamic range of oscillations of the laser outputs. Each of the three total signals consisting of the chaotic output and the message encoded on it are transmitted simultaneously to the two other lasers. The transmitted signals are received and decoded at the three receivers. Figs. 12–14 show the original and decoded waveforms of the above audio signals. Fig. 12(a), (b) and (c) show the original signal  $M_1$  encoded and transmitted by laser  $L_1$ ,  $M_1$  decoded at  $L_2$  and  $M_1$  decoded at  $L_3$  respectively. Figs. 13(a)–(c) and 14(a)–(c) show the corresponding waveforms of messages  $M_2$  and  $M_3$  respectively. It can be observed from these figures that the decoded messages have the same waveforms as their original counterparts. These decoded signals are converted to wave files which are played back with full clarity.

The performance of the above scheme for digital signals in a noisy channel is investigated using bit-error-rate (BER). The message signals are contaminated by additive Gaussian noise of strength ‘ $n$ ’ and the variation of BER versus (energy per bit/noise spectral density) evaluated as  $E_b/N_o = B^2 T_b / (n^2) T_s$  [39,40] is plot-

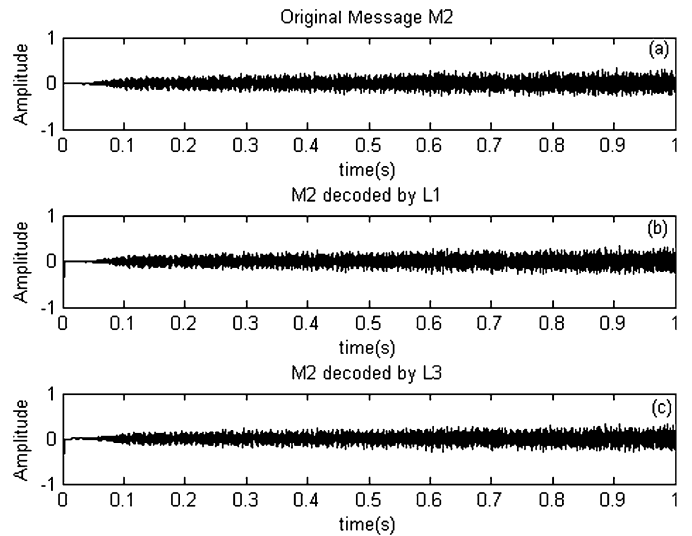


**Fig. 13.** (a) Waveforms of original audio signal of toy train horn which is encoded as message  $M_2$  onto the chaotic output of the laser  $L_2$ . (b) Waveform of  $M_2$  decoded at  $L_1$ . (c) Waveform of  $M_2$  decoded at  $L_3$ .

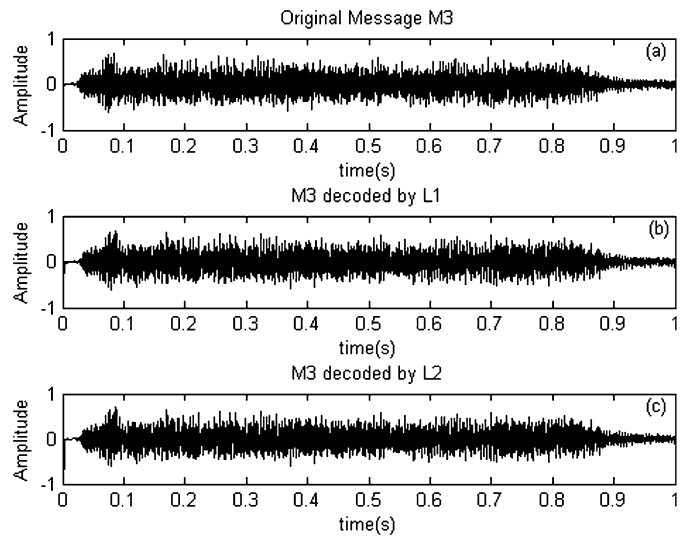


**Fig. 14.** (a) Waveforms of original audio signal of air horn which is encoded as message  $M_3$  onto the chaotic output of the laser  $L_1$ . (b) Waveform of  $M_3$  decoded at  $L_1$ . (c) Waveform of  $M_3$  decoded at  $L_2$ .

ted in Fig. 15(a)–(f). The message signals are sampled at every  $T_s$  which is kept same as the time step of evolution of the laser and are averaged over a bit time  $T_b$ . Depending on this average, the bits are evaluated as a ‘zero’ or ‘one’. Fig. 15 shows the results for bit size of  $B = 0.0001$  and  $T_b/T_s = 10$ . The dynamics of each element is determined by its self feedback and the coupling received by the other two elements. Thus any attacker who breaks into the communication channel need to have information regarding each of the signals for exact reconstruction of the decoding wave. However, further detailed investigations are necessary for providing information regarding the level of security.

#### 4. Conclusions

The method of adding a delayed coupling together with the delayed self optoelectronic feedback is applied effectively to achieve isochronal synchronisation between the elements of an array of three mutually coupled directly modulated semiconductor lasers.

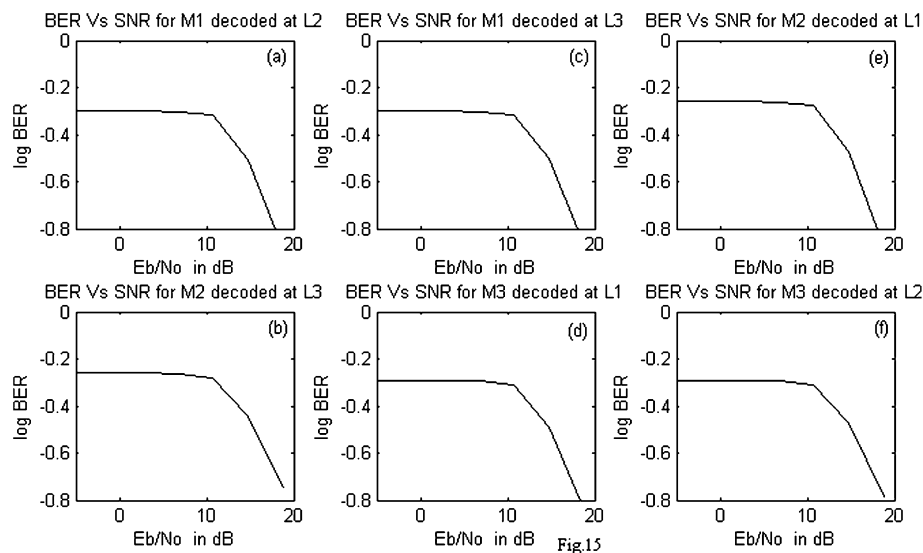


**Fig. 15.** Variation of BER with respect to noise density calculated for messages transmitted and decoded simultaneously for (a) message  $M_1$  decoded at  $L_2$ ; (b) message  $M_1$  decoded at  $L_3$ ; (c) message  $M_2$  decoded at  $L_1$ ; (d) message  $M_2$  decoded at  $L_3$ ; (e) message  $M_3$  decoded at  $L_1$ ; (f) message  $M_3$  decoded at  $L_2$ .

The isochronal synchronisation achieved is thereby used for simultaneous multi-user bidirectional secure communication. Using this method, three messages can be simultaneously transmitted between three mutually coupled directly modulated semiconductor lasers. Thus a single element can transmit its message to two different receivers and at the same time can receive two messages from two other elements. This method of sending and receiving messages encoded on chaotic carriers using an array of three lasers can be suitably extended to arrays of lasers with more number of elements. This possibility of simultaneous multi-user secure communication will be a new direction in the field of optical cryptographic communication in public channel networks.

### Acknowledgements

One of the authors (B.M.K.) would like to acknowledge with thanks the financial support from the Department of Science and Technology (Govt. of India), through Fast Track Scheme for Young Scientists, No. SR/FTP/PS-14/2004, Prof. Jacob Philip, Director, STIC for technical support, Prof. R. Pratap, International School of Photonics, Cochin University of Science and Technology and Dr. S. Sivaprakasam, University of Pondicherry, for fruitful discussions.

### References

- [1] G.D. VanWiggeren, R. Roy, *Science* 279 (1998) 1198.
- [2] I. Schreiber, M. Marek, *Physica D* 5 (1982) 258.
- [3] S.K. Han, D. Kuerrer, K. Kuramoto, *Phys. Rev. Lett.* 75 (1995) 3190.
- [4] C.R. Mirasso, R. Vincete, P. Colet, J. Mullet, T. Perez, C. R. Phys. 5 (2004) 613.
- [5] L. Larger, G. Goedgebuer, C. R. Phys. 5 (2004) 609.
- [6] P. Colet, R. Roy, *Opt. Lett.* 19 (1994) 2056.
- [7] J. Ohtsubo, *IEEE J. Quantum Electron.* 38 (2002) 1141.
- [8] J.P. Goedgebuer, L. Larger, H. Porte, *Phys. Rev. Lett.* 80 (1998) 2249.
- [9] M.R. Parvathi, Bindu M. Krishna, S. Rajesh, M.P. John, V.M. Nandakumaran, *Phys. Lett. A* 373 (2008) 96.
- [10] M.R. Parvathi, Bindu M. Krishna, S. Rajesh, M.P. John, V.M. Nandakumaran, *Chaos Solitons Fractals* 42 (2009) 515.
- [11] A. Argyris, D. Syvridis, L. Larger, V.A. Lodi, P. Colet, I. Fischer, J. García-Ojalvo, C.R. Mirasso, L. Pesquera, K.A. Shore, *Nature* 438 (2005) 343.
- [12] G.P. Agrawal, *Appl. Phys. Lett.* 49 (1986) 1013.
- [13] T. Kuruvilla, V.M. Nandakumaran, *Phys. Lett. A* 254 (1999) 59.
- [14] V. Bindu, V.M. Nandakumaran, *Phys. Lett. A* 227 (2000) 345.
- [15] V. Bindu, V.M. Nandakumaran, *J. Opt. A: Pure Appl. Opt.* 4 (2002) 115.
- [16] Bindu M. Krishna, Manu P. John, V.M. Nandakumaran, *Pramana* 71 (2008) 1259.
- [17] H.F. Liu, W.F. Ngai, *IEEE J. Quantum Electron.* 29 (1993) 1668.
- [18] T.H. Yoon, C.H. Lee, S.Y. Shin, *IEEE J. Quantum Electron.* 25 (1989) 1993.
- [19] Y.G. Zhao, *IEEE J. Quantum Electron.* 28 (1992) 2009.
- [20] C.G. Lim, S. Iezekiel, C.M. Snowden, *Appl. Phys. Lett.* 78 (2001) 2384.
- [21] E.F. Manffra, I.L. Caldas, R.L. Viana, H.J. Kalinowski, *Nonlinear Dyn.* 27 (2002) 185.
- [22] S. Rajesh, V.M. Nandakumaran, *Phys. Lett. A* 319 (2003) 340.
- [23] S. Rajesh, V.M. Nandakumaran, *Physica D* 213 (2006) 113.
- [24] Y. Liu, P. Davis, Y. Takiguchi, T. Aida, A. Saito, J.M. Liu, *IEEE J. Quantum Electron.* 39 (2003) 269.
- [25] A. Uchida, Y. Liu, I. Fischer, P. Davis, T. Aida, *Phys. Rev. A* 64 (2001) 023801.
- [26] T. Heil, I. Fischer, W. Elsässer, J. Mulet, C.R. Mirasso, *Phys. Rev. Lett.* 86 (2001) 795.
- [27] D.M. Kane, J.P. Toomey, M.W. Lee, K.A. Shore, *Opt. Lett.* 31 (2006) 20.
- [28] S. Tang, J.M. Liu, *Phys. Rev. Lett.* 90 (2003) 194101.
- [29] S. Tang, J.M. Liu, *IEEE J. Quantum Electron.* 39 (2003) 963.
- [30] A. Wagemakers, J.M. Buldú, M.A.F. Sanjuan, *Chaos* 17 (2007) 023128.
- [31] A.S. Landman, I.B. Shwartz, *Phys. Rev. E* 75 (2007) 026201.
- [32] A. Wagemakers, J.M. Buldú, M.A.F. Sanjuan, *Europhys. Lett.* 81 (2008) 40005.
- [33] I. Fischer, R. Vincete, J.M. Buldú, M. Peil, C.R. Mirasso, M.C. Torrent, J. García-Ojalvo, *Phys. Rev. Lett.* 97 (2006) 123902.
- [34] E. Klein, N. Gross, M. Rosenbluh, W. Kinzel, L. Khaykovich, I. Kanter, *Phys. Rev. E* 73 (2006) 066214.
- [35] R. Vincete, S. Tang, J. Mulet, C.R. Mirasso, J.-M. Liu, *Phys. Rev. E* 73 (2006) 047201.
- [36] I.B. Shwartz, L.B. Shaw, *Phys. Rev. E* 75 (2007) 046207.
- [37] B.B. Zhou, R. Roy, *Phys. Rev. E* 75 (2007) 026205.
- [38] N. Gross, W. Kinzel, I. Kanter, M. Rosenbluh, L. Klykovich, *Opt. Commun.* 267 (2006) 464.
- [39] H.D.I. Abarbanel, M.B. Kennel, L. Illing, S. Tang, H.F. Chen, J.M. Liu, *IEEE J. Quantum Electron.* 37 (2001) 1301.
- [40] S. Tang, H.F. Chen, S.K. Hwang, J.M. Liu, *IEEE Trans. Circuits Syst. I* 49 (2002) 163.